Improved ZZ a posteriori error estimators for diffusion problems: Discontinuous elements

Zhiqiang Cai [a,1], Cuiyu He [b,*], Shun Zhang [c,2]

[a] *Department of Mathematics, Purdue University, 150 N. University Street, West Lafayette, IN 47907-2067, United States of America*
[b] *Department of Mathematics, University of Georgia, 1023 D.W. Brooks Dr, Athens, GA, 30606, United States of America*
[c] *Department of Mathematics, City University of Hong Kong, Hong Kong*

ARTICLE INFO

ABSTRACT

In Cai, He, and Zhang (2017), we studied an improved Zienkiewicz-Zhu (ZZ) a posteriori error estimator for conforming linear finite element approximation to diffusion problems. The estimator is more efficient than the original ZZ estimator for non-smooth problems, but with comparable computational costs. This paper extends the improved ZZ estimator for discontinuous linear finite element approximations including both nonconforming and discontinuous elements. In addition to post-processing a flux, we further explicitly recover a gradient in the $H(\mathrm{curl})$ conforming finite element space. The resulting error estimator is proved, theoretically and numerically, to be efficient and reliable with constants independent of the jump of the coefficient regardless of its distribution.

© 2020 IMACS. Published by Elsevier B.V. All rights reserved.

1. Introduction

By recovering a gradient/flux in the conforming C^0 linear vector finite element space from the numerical gradient/flux, the recovery type Zienkiewicz-Zhu (ZZ) a posteriori error estimator (see [29]) is defined as the L^2 norm of the difference between the recovered and the numerical gradients/fluxes. Since its introduction in 1987, the ZZ estimator has been widely adopted in the engineering practice and has been the subject of mathematical study due to its simplicity, generality, and asymptotic exactness (see, e.g., [11,18,23–28,30,31]). However, it is also well known that the ZZ estimator is inefficient for non-smooth problems. The counterexamples in [5] for elliptic interface problems show that the ZZ estimator is arbitrarily large while the true error is zero. We identify the problem for ZZ error estimator is that it recovers both the gradient and flux in the H^1 space while the flux and gradient only belongs to $H(\mathrm{div})$ and $H(\mathrm{curl})$ spaces, respectively.

For the conforming finite element approximation, to circumvent this drawback of the ZZ estimator, we can simply recover a flux in the $H(\mathrm{div})$ conforming finite element space such as the Raviart-Thomas (RT) or Brezzi-Douglas-Marini (BDM) elements by a global L^2 projection (see [8]). This recovery procedure is further simplified by an explicit scheme developed recently in [5] and applicable to problems with full diffusion tensor. The resulting (improved ZZ) estimator is shown to be efficient and reliable theoretically and numerically for interface problems. Moreover, the efficiency and reliability constants are independent of the jump of the diffusion coefficients provided that the distribution of the coefficient is quasi-monotone.

---

* Corresponding author.
E-mail addresses: caiz@purdue.edu (Z. Cai), cuiyu.he@uga.edu (C. He), shun.zhang@cityu.edu.hk (S. Zhang).

For the nonconforming and discontinuous linear finite element approximations, it is well known that flux recovery is not sufficient since the numerical solution is "broken", i.e., not in the H^1 space. Therefore, in addition to the flux recovery, one needs either recover a gradient in the $H(\text{curl})$ conforming finite element space in [9,7] or a solution in the H^1 space [1,2] for the nonconforming and discontinuous linear finite element approximations. We note that the recovery procedures in [9,7] consist of both implicit and explicit schemes. The implicit one requires to solve a global L^2 projection (which is computationally costive), while the explicit one (with computation cost comparative to ZZ) is limited to the piecewise "constant" vector space for the gradient and to scaler diffusion coefficient.

The purpose of this paper is to employ the general approach introduced in [5] to explicitly construct a gradient in the $H(\text{curl}; \Omega)$ conforming subspace of either the piecewise "constant" or the higher order vector spaces for the diffusion problem with both scaler and full tensor diffusion coefficient. In this paper, these spaces are chosen as the $H(\text{curl}; \Omega)$ conforming first and second types of Nédélec spaces. Also, the diffusion coefficient could undergo large jumps across interfaces. With the recovered gradients and fluxes, the improved ZZ estimators then consist of two parts measuring the so-called conforming and nonconforming errors. The error estimators are further analyzed by establishing their global reliability and local efficiency bounds.

We note that both the reliability and the efficiency constants for the error estimators are theoretically proved independent of the jump of the diffusion coefficients. Moreover, unlike the conforming case which requires the quasi-monotone assumption [21] to ensure the robustness, we are able to prove the same robust result regardless the distribution of the coefficient. The first robustness result without restrictive assumption was proved in [4] for the residual type a posteriori error estimators of nonconforming and DG finite element methods. In this paper, we prove the same unconditional robustness for our recovery type a posteriori error estimation.

Compared with the classical residual-based error estimation, one main advantage of the recovery-type a posteriori error estimation is the asymptotic exactness when the mesh is fine enough. It is well known that residual-type error estimator [6,22,13] does not share asymptotic exactness and often the constants are polynomial order dependent. In the last decade, the equilibrate-type error estimation with guaranteed upper bound (reliability constant is one and thus polynomial order robust) was intensively explored, see [1,2,16,19,17]. To ensure the reliability constant being one, the equilibrate-type error estimator usually recovers a H^1 function for the nonconforming error. This applied to the diffusion problem will result in the fact that constants can only proved to be robust with respect to the jump of the diffusion coefficient when it is quasi-monotone. We note that to ensure the guaranteed upper bound for the nonconforming error, one can also recover a gradient that is curl free. In principle, we can apply the methods introduced in [10,17] to obtain such a gradient. However, this requires to solve local implicit star-patch problems and therefore increases algorithmic complexity.

Thanks to its generality, our idea serves as a good candidate for the development of the recovery type explicit a posteriori error estimation for higher order finite elements and non-simplicial meshes, e.g., quad-meshes with hanging nodes. Moreover, the idea can be easily adapted to other types of finite element methods.

Numerical results for the Kellogg test problem and a *L*-shape Poisson problem are presented to verify our theoretically results.

This paper is organized as follows. Section 2 describes both nonconforming and discontinuous Galerkin finite element approximations to diffusion problems. The improved ZZ a posteriori error estimators are introduced in Section 3 and the reliability and efficiency bounds independent of the jump of coefficients are established in Section 4. In Section 5, we provide explicit formulas for the recovered flux and gradient. Finally, the numerical results are presented in Section 6.

2. Finite element approximations to diffusion problem

Let Ω be a bounded polygonal domain in $\mathbf{R}^2$, with boundary $\partial\Omega = \overline{\Gamma}_D \cup \overline{\Gamma}_N$, $\Gamma_D \cap \Gamma_N = \emptyset$, meas$(\Gamma_D) \neq 0$, and let $\mathbf{n}$ be the outward unit vector normal to the boundary. Consider diffusion problem

$$-\nabla \cdot (A(x)\nabla u) = f \quad \text{in } \Omega \tag{2.1}$$

with boundary conditions

$$-A\nabla u \cdot \mathbf{n} = g_N \quad \text{on } \Gamma_N \quad \text{and} \quad u = g_D \quad \text{on } \Gamma_D, \tag{2.2}$$

where the $\nabla\cdot$ and ∇ are the divergence and gradient operators, respectively; $f \in L^2(\Omega)$, $g_N \in H^{-1/2}(\Gamma_N)$, $g_D \in H^{1/2}(\Gamma_D)$; and A is a piecewise symmetric, positive and definite tensor function. In this paper, we restrict our discussion in two dimensions for notation simplicity. The algorithm and analysis can be extended to three dimensions.

Let

$$H_{g,D}^1(\Omega) = \left\{ v \in H^1(\Omega) : v = g_D \text{ on } \Gamma_D \right\} \quad \text{and} \quad H_D^1(\Omega) = H_{0,D}^1(\Omega).$$

Then the corresponding variational problem of (2.1) is to find $u \in H_{g,D}^1(\Omega)$ such that

$$a(u, v) := (A\nabla u, \nabla v) = f(v), \quad \forall v \in H_D^1(\Omega) \tag{2.3}$$

with the linear form $f(v) := (f, v) - (g_N, v)_{\Gamma_N}$, where $(\cdot, \cdot)_\omega$ is the L^2 inner product over the domain ω. The subscript ω is omitted when $\omega = \Omega$.

Let $\mathcal{T} = \{K\}$ be a triangulation of the domain Ω with only triangular elements and denote by h_K the diameter of the element K. Assume that the triangulation is regular and that the physical interfaces

$$\Gamma := \left\{ \partial\Omega_i \cap \partial\Omega_j : i, j = 1, \cdots, n \right\}$$

do not cut through any element $K \in \mathcal{T}$, where $\{\Omega_i\}_{i=1}^n$ are disjoint polygonal subdomains of Ω such that $\bar{\Omega} = \cup_{i=1}^n \bar{\Omega}_i$.

For simplicity, with respect to $\mathcal{T}$, assume that f is a piecewise constant function on Ω, that g_D is piecewise affine on Γ_D, and that g_N is piecewise constant on Γ_N. Furthermore, assume that A is locally and mildly anisotropic in the sense that there exists a moderate size constant $\kappa > 0$ such that

$$\frac{\lambda_{\max, K}}{\lambda_{\min, K}} \leq \kappa, \quad \forall\, K \in \mathcal{T}, \tag{2.4}$$

where $\lambda_{\max, K}$ and $\lambda_{\min, K}$ are the respective maximal and minimal eigenvalues of $A_K := A\big|_K$. Note that this assumption permits possible large value of $\lambda_{max}/\lambda_{min}$, where λ_{max} and λ_{min} are the respective global maximal and minimal eigenvalues of A. We note that the simplified assumption on data can be extended to generic cases with extra data oscillation terms in the error analysis. Moreover, the oscillation terms will be of higher order when the data functions possess proper regularity.

Denote the set of all vertices of the triangulation by $\mathcal{N} := \mathcal{N}_I \cup \mathcal{N}_D \cup \mathcal{N}_N$, where $\mathcal{N}_I$ is the set of all interior nodes and $\mathcal{N}_D$ and $\mathcal{N}_N$ are the sets of all boundary vertices belonging to the respective $\overline{\Gamma}_D$ and Γ_N. Denote the set of all edges of the triangulation by $\mathcal{E} := \mathcal{E}_I \cup \mathcal{E}_D \cup \mathcal{E}_N$, where $\mathcal{E}_I$ is the set of all interior element edges and $\mathcal{E}_D$ and $\mathcal{E}_N$ are the sets of all boundary edges belonging to the respective Γ_D and Γ_N. For each $F \in \mathcal{E}_I$, denote by $\mathbf{n}_F := (n_{1,F}, n_{2,F})^t$ an unit vector normal to F; then $\mathbf{t}_F = (-n_{2,F}, n_{1,F})^t$ is an unit vector tangent to F; let K_F^- and K_F^+ be the two elements sharing the common edge F such that the unit outward vector normal to ∂K_F^- coincides with $\mathbf{n}_F$. For each $F \in \mathcal{E}_D \cup \mathcal{E}_N$, $\mathbf{n}_F$ is the unit outward vector normal to $\partial\Omega$ and denote the element by K_F^-. For each $K \in \mathcal{T}$ denote by h_K the diameter of K and by $\mathcal{E}_K$ and $\mathcal{N}_K$ the set of all edges and vertices of K, respectively.

Denote the Crouziex-Raviart (CR) nonconforming finite element space [15] by

$$S^{cr}(\mathcal{T}) = \left\{ v \in L^2(\Omega) : v|_K \in \mathbb{P}_1(K),\ \forall K \in \mathcal{T},\ \text{and} \int_F [\![v]\!]_F\, ds = 0,\ \forall F \in \mathcal{E}_I \right\},$$

where $\mathbb{P}_k(K)$ is the space of polynomial of order not greater than k on the element K, $[\![\cdot]\!]_F$ is the jump over edge F defined by $[\![v]\!]_F = v_F^- - v_F^+$ for all $F \in \mathcal{E}_I$ and v_F^- for all $F \in \mathcal{E}_D \cup \mathcal{E}_N$ and $v_F^\pm := (v|_{K_F^\pm})|_F$. Also let

$$S_{g,D}^{cr}(\mathcal{T}) = \left\{ v \in S^{cr}(\mathcal{T}) : \int_F v\, ds = \int_F g_D ds,\ \forall F \in \mathcal{E}_D \right\}.$$

The nonconforming finite element approximation is to find $u^{cr} \in S_{g,D}^{cr}$ such that

$$(A \nabla_h u^{cr}, \nabla_h v) = (f, v) - (g_N, v)_{\Gamma_N}, \quad \forall v \in S_{0,D}^{cr}(\mathcal{T}), \tag{2.5}$$

where ∇_h is the discrete gradient operator, i.e., $(\nabla_h v)|_K = \nabla(v|_K)$ for all $K \in \mathcal{T}$.

In the remainder of this section, we describe discontinuous Galerkin finite element method using notations in [7]. To this end, for each element $K \in \mathcal{T}$, define a function α_K on $\mathcal{E}_K$ such that

$$\alpha_K(F) = \mathbf{n}_F^t (A|_K) \mathbf{n}_F, \quad \forall K \in \mathcal{T}.$$

It is obvious that $\lambda_{\min, K} \leq \alpha_K(F) \leq \lambda_{\max, K}$ for all $F \in \mathcal{E}_K$. Due to the mildly anisotropic assumption, other choices of $\alpha_K(F)$ in the interval $[\lambda_{\min, K}, \lambda_{\max, K}]$ will not affect the robustness of our methods. The reason of choosing the current version instead of the minimum or maximum eigenvalue is that it can be computed explicitly.

For each $F \in \mathcal{E}_I$, let $\alpha_F^\pm = \alpha_{K_F^\pm}(F)$, and w_F^+ and w_F^- be weights defined on F such that

$$w_F^\pm = \frac{\alpha_F^\mp}{\alpha_F^- + \alpha_F^+}. \tag{2.6}$$

Define the following weighted averages

$$\{v(x)\}_w^F = \begin{cases} w_F^- v_F^- + w_F^+ v_F^+ & \text{for } F \in \mathcal{E}_I, \\ v|_F^- & \text{for } F \in \mathcal{E}_D \cup \mathcal{E}_N \end{cases} \quad \text{and} \quad \{v(x)\}_F^w = \begin{cases} w_F^+ v_F^- + w_F^- v_F^+ & \text{for } F \in \mathcal{E}_I, \\ 0 & \text{for } F \in \mathcal{E}_D \cup \mathcal{E}_N \end{cases}.$$

The notations of $\{\}_w^F$ and $\{\}_F^w$ will be replaced by the respective $\{\}_w$ and $\{\}^w$ when the indication of F is obvious. It is easy to verify that

$$[\![vw]\!]_F = \{v\}_w [\![w]\!] + [\![v]\!] \{v\}^w.$$

Denote the arithmetic and harmonic averages of $\{\alpha_F^+, \alpha_F^-\}$ on $F \in \mathcal{E}$ by

$$\alpha_{F,A} = \begin{cases} \dfrac{\alpha_F^+ + \alpha_F^-}{2} & F \in \mathcal{E}_I, \\[2mm] \alpha_F^- & F \in \mathcal{E}_D, \end{cases} \quad \text{and} \quad \alpha_{F,H} = \begin{cases} \dfrac{2\alpha_F^+ \alpha_F^-}{\alpha_F^+ + \alpha_F^-}, & F \in \mathcal{E}_I, \\[2mm] \alpha_F^- & F \in \mathcal{E}_D, \end{cases}$$

respectively, which are equivalent to its respective maximum and minimum.

Denote the discontinuous finite element space of the first order on the triangulation $\mathcal{T}$ by

$$S^{dg}(\mathcal{T}) = \left\{ v \in L^2(\Omega) : v|_K \in \mathbb{P}_1(K) \quad \forall K \in \mathcal{T} \right\}.$$

The discontinuous Galerkin finite element method is to seek $u^{dg} \in S^{dg}(\mathcal{T})$ such that

$$a_{dg}(u^{dg}, v) = f(v) \quad \forall v \in S^{dg}(\mathcal{T}) \tag{2.7}$$

where the bilinear form $a_{dg}(\cdot, \cdot)$ is given by

$$\begin{aligned} a_{dg}(u, v) =& (A\nabla_h u, \nabla_h v) + \sum_{F \in \mathcal{E}_I \cup \mathcal{E}_D} \int_F \gamma \frac{\alpha_{F,H}}{h_F} [\![u]\!][\![v]\!] \, ds \\ & - \sum_{F \in \mathcal{E}_I \cup \mathcal{E}_D} \int_F \{A\nabla u \cdot \mathbf{n}_F\}_w [\![v]\!] ds - \sum_{F \in \mathcal{E}_I \cup \mathcal{E}_D} \int_F \{A\nabla v \cdot \mathbf{n}_F\}_w [\![u]\!] ds, \end{aligned} \tag{2.8}$$

and the linear form $f(\cdot)$ is given by

$$f(v) = (f, v) + \sum_{F \in \mathcal{E}_D} \gamma \frac{\alpha_{F,H}}{h_F} \int_F g_D v \, ds - \sum_{F \in \mathcal{E}_D} \int_F g_D \left(A\nabla v \cdot \mathbf{n}_F \right) ds - \sum_{F \in \mathcal{E}_N} \int_F g_N v \, ds.$$

The γ is a positive constant that is large enough and only depending on the shape of elements.

According to [7], the exact solution of (2.3) satisfies the equation (2.7). Hence we have the following error equation:

$$a_{dg}(u - u^{dg}, v) = 0 \quad \forall v \in S^{dg}(\mathcal{T}). \tag{2.9}$$

Define the jump semi-norm and the DG norm by

$$|v|_{J,F} = \sqrt{\frac{\alpha_{F,H}}{h_F}} \| [\![v]\!] \|_{0,F} \quad \text{and} \quad \|v\|_{dg} = \left(\|A^{1/2} \nabla_h v\|_{0,\Omega}^2 + \sum_{F \in \mathcal{E}} |v|_{J,F}^2 \right)^{1/2}.$$

3. Improved ZZ estimator

In this section, we set up the framework for the gradient recovery. We refer to [5] for the flux recovery. In two dimensions, for a vector-valued function $\boldsymbol{\tau} = (\tau_1, \tau_2)$, define the divergence and curl operators by

$$\nabla \cdot \boldsymbol{\tau} = \frac{\partial \tau_1}{\partial x_1} + \frac{\partial \tau_2}{\partial x_2} \quad \text{and} \quad \nabla \times \boldsymbol{\tau} = \frac{\partial \tau_2}{\partial x_1} - \frac{\partial \tau_1}{\partial x_2},$$

respectively. For a scaler-valued function v, define the adjoint curl operator $\nabla^\perp$ by

$$\nabla^\perp v = Q \nabla v = \left(-\frac{\partial v}{\partial x_2}, \frac{\partial v}{\partial x_1} \right)^t \quad \text{with} \quad Q = \begin{bmatrix} 0 & -1 \\ 1 & 0 \end{bmatrix}.$$

We shall use the following Hilbert spaces:

$$H(\text{div}; \Omega) = \left\{ \boldsymbol{\tau} \in L^2(\Omega)^2 : \nabla \cdot \boldsymbol{\tau} \in L^2(\Omega) \right\} \quad \text{and} \quad H(\text{curl}; \Omega) = \left\{ \boldsymbol{\tau} \in L^2(\Omega)^2 : \nabla \times \boldsymbol{\tau} \in L^2(\Omega) \right\}$$

equipped with the norms

$$\|\boldsymbol{\tau}\|_{H(\text{div}; \Omega)} = \left(\|\boldsymbol{\tau}\|_{0,\Omega}^2 + \|\nabla \cdot \boldsymbol{\tau}\|_{0,\Omega}^2 \right)^{1/2} \quad \text{and} \quad \|\boldsymbol{\tau}\|_{H(\text{curl}; \Omega)} = \left(\|\boldsymbol{\tau}\|_{0,\Omega}^2 + \|\nabla \times \boldsymbol{\tau}\|_{0,\Omega}^2 \right)^{1/2},$$

respectively. Note that $H^1(\Omega)^2 \subset H(\text{div}; \Omega) \cap H(\text{curl}; \Omega)$ and that the inverse inclusion is valid only for the convex domain or the domain with smooth boundary [14]. Let

$$H_{g,N}(\text{div}; \Omega) = \{\boldsymbol{\tau} \in H(\text{div}; \Omega) : \boldsymbol{\tau} \cdot \mathbf{n}|_F = g_N, \quad \forall F \in \mathcal{E}_N\}$$

and

$$H_{g,D}(\text{curl}; \Omega) = \{\boldsymbol{\tau} \in H(\text{curl}; \Omega) : \boldsymbol{\tau} \cdot \mathbf{t}|_F = \partial g_D/\partial t, \quad \forall F \in \mathcal{E}_D\}.$$

3.1. Gradient recovery

Denote the $H(\text{curl}; \Omega)$ conforming first and second types of Nédélec spaces of the lowest order by

$$\text{NE} = \{\boldsymbol{\tau} \in H(\text{curl}; \Omega) : \boldsymbol{\tau}|_K \in \text{NE}(K), \quad \forall K \in \mathcal{T}\},$$

$$\text{and } \text{ND} = \{\boldsymbol{\tau} \in H(\text{curl}; \Omega) : \boldsymbol{\tau}|_K \in \text{ND}(K), \quad \forall K \in \mathcal{T}\},$$

respectively, where $\text{NE}(K) = \mathbb{P}_0(K)^2 + (x_2, -x_1)\mathbb{P}_0(K)$ and $\text{ND}(K) = \mathbb{P}_1(K)^2$. Let

$$\text{NE}_{g,D} = \{\boldsymbol{\tau} \in \text{NE} : \boldsymbol{\tau} \cdot \mathbf{t}_F|_F = g'_{D,F}, \quad \forall F \in \mathcal{E}_D\},$$

$$\text{and } \text{ND}_{g,D} = \{\boldsymbol{\tau} \in \text{ND} : \boldsymbol{\tau} \cdot \mathbf{t}_F|_F = g'_{D,F}, \quad \forall F \in \mathcal{E}_D\},$$

where $g'_{D,F} := \partial(g_D|_F)/\partial t$.

For each edge $F \in \mathcal{E}$, denote by $\mathbf{s}_F$ and $\mathbf{e}_F$ the globally fixed initial and terminal points of F, respectively, such that $\mathbf{e}_F - \mathbf{s}_F = |F|\mathbf{t}_F$. Denote by $\boldsymbol{\zeta}_F$ the global nodal basis function of NE associated with F such that

$$(\boldsymbol{\zeta}_F \cdot \mathbf{t}_{F'})|_{F'} = \delta_{FF'}|F|^{-1}, \quad \forall F' \in \mathcal{E} \tag{3.10}$$

and by $\boldsymbol{\xi}_{s,F}$ and $\boldsymbol{\xi}_{e,F}$ the global basis functions of ND associated with F satisfying

$$(\boldsymbol{\xi}_{s,F} \cdot \mathbf{t}_{F'})|_{F'} = \delta_{FF'}|F|^{-1}\lambda_{\mathbf{s}_F} \quad \text{and} \quad (\boldsymbol{\xi}_{e,F} \cdot \mathbf{t}_{F'})|_{F'} = \delta_{FF'}|F|^{-1}\lambda_{\mathbf{e}_F}, \tag{3.11}$$

respectively, where δ is the Kronecker delta function and λ is the barycentric basis function. For each $F \in \mathcal{E}$, define

$$\text{NE}_F = \text{span}\{\boldsymbol{\zeta}_F\} \quad \text{and} \quad \text{ND}_F = \text{span}\{\boldsymbol{\xi}_{s,F}, \boldsymbol{\xi}_{e,F}\}.$$

Since $g'_{D,F}$ is piecewise constant on Γ_D, for any $\boldsymbol{\tau} \in \text{ND}_{g,D}$ or $\text{NE}_{g,D}$, it can be written as

$$\boldsymbol{\tau} = \sum_{F \in \mathcal{E}_I \cup \mathcal{E}_N} \boldsymbol{\tau}_F + \sum_{F \in \mathcal{E}_D} g'_{D,F}|F|\boldsymbol{\zeta}_F \quad \text{with } \boldsymbol{\tau}_F \in \text{ND}_F \text{ or } \text{NE}_F. \tag{3.12}$$

Given the numerical solution, denoted by $u_{\mathcal{T}} := u^{cr}$ or u^{dg}, define its numerical gradient by $\tilde{\boldsymbol{\rho}}_{\mathcal{T}} = \nabla_h u_{\mathcal{T}}$. For any $K \in \mathcal{T}$, the restriction of $\tilde{\boldsymbol{\rho}}_{\mathcal{T}}$ on K is a constant vector and therefore has the following representation in $\text{NE}(K)$:

$$\tilde{\boldsymbol{\rho}}_{\mathcal{T}}|_K = \sum_{F \in \mathcal{E}K} \tilde{\rho}_{F,K}|F|(\boldsymbol{\zeta}_F|_K),$$

where $\tilde{\rho}_{F,K} := (\tilde{\boldsymbol{\rho}}_{\mathcal{T}}|_K \cdot \mathbf{t}_F)|_F$ is the tangential component of $\tilde{\boldsymbol{\rho}}_{\mathcal{T}}|_K$ on F. On each interior edge $F \in \mathcal{E}_I$, the tangential component of the numerical gradient has two values

$$\tilde{\rho}_F^- := \tilde{\rho}_{F,K_F^-} \quad \text{and} \quad \tilde{\rho}_F^+ := \tilde{\rho}_{F,K_F^+}.$$

Denote by $\boldsymbol{\zeta}_F^-$ and $\boldsymbol{\zeta}_F^+$ the restriction of $\boldsymbol{\zeta}_F$ on K_F^- and K_F^+, respectively. Then the numerical gradient also has the following edge representation:

$$\tilde{\boldsymbol{\rho}}_{\mathcal{T}} = \sum_{F \in \mathcal{E}} \tilde{\boldsymbol{\rho}}_F \quad \text{with} \quad \tilde{\boldsymbol{\rho}}_F = \begin{cases} \tilde{\rho}_F^-|F|\boldsymbol{\zeta}_F^- + \tilde{\rho}_F^+|F|\boldsymbol{\zeta}_F^+, & \forall F \in \mathcal{E}_I, \\ \tilde{\rho}_F^-|F|\boldsymbol{\zeta}_F^-, & \forall F \in \mathcal{E}_D \cup \mathcal{E}_N. \end{cases} \tag{3.13}$$

For any $\boldsymbol{\tau} \in \text{NE}_{g,D}$ or $\text{ND}_{g,D}$, (3.12) and (3.13) give

$$\boldsymbol{\tau} - \tilde{\boldsymbol{\rho}}_{\mathcal{T}} = \sum_{F \in \mathcal{E}_I} \left(\boldsymbol{\tau}_F - \tilde{\boldsymbol{\rho}}_F\right) + \sum_{F \in \mathcal{E}_N} \left(\boldsymbol{\tau}_F - \tilde{\rho}_F^-|F|\boldsymbol{\zeta}_F^-\right) + \sum_{F \in \mathcal{E}_D} \left(g'_{D,F} - \tilde{\rho}_F^-\right)|F|\boldsymbol{\zeta}_F^-,$$

which, together with the triangle inequality and the choice of $\boldsymbol{\tau}_F = \tilde{\rho}_F^-|F|\boldsymbol{\zeta}_F^-$ for all $F \in \mathcal{E}_N$, implies

$$\min_{\boldsymbol{\tau} \in \mathcal{V}_{g,D}} \left\| A^{1/2} \left(\boldsymbol{\tau} - \tilde{\boldsymbol{\rho}}_{\mathcal{T}} \right) \right\|_{0,\Omega} \le \sum_{F \in \mathcal{E}_I} \min_{\boldsymbol{\tau} \in \mathcal{V}_F} \left\| A^{1/2} \left(\boldsymbol{\tau} - \tilde{\boldsymbol{\rho}}_F \right) \right\|_{0,\omega_F} + \sum_{F \in \mathcal{E}_D} \left\| A^{1/2} \left(g'_{D,F} - \tilde{\rho}_F^- \right) |F| \boldsymbol{\zeta}_F^- \right\|_{0,K_F^-}, \tag{3.14}$$

where $\mathcal{V} = \text{NE}$ or ND and $\omega_F = K_F^+ \cup K_F^-$.

For each $F \in \mathcal{E}_I$, let $\hat{\boldsymbol{\rho}}_F \in \mathcal{V}_F = \text{NE}_F$ or ND_F be the solution of the following local minimization problem, i.e.,

$$\left\| A^{1/2} \left(\hat{\boldsymbol{\rho}}_F - \tilde{\boldsymbol{\rho}}_F \right) \right\|_{0,\omega_F} = \min_{\boldsymbol{\tau} \in \mathcal{V}_F} \left\| A^{1/2} \left(\boldsymbol{\tau} - \tilde{\boldsymbol{\rho}}_F \right) \right\|_{0,\omega_F}, \tag{3.15}$$

and, on the boundary edges, define

$$\hat{\boldsymbol{\rho}}_F = \begin{cases} \tilde{\boldsymbol{\rho}}_F, & \forall F \in \mathcal{E}_N, \\ g'_{D,F} |F| \boldsymbol{\zeta}_F^-, & \forall F \in \mathcal{E}_D. \end{cases}$$

Finally we define the recovered gradient $\hat{\boldsymbol{\rho}}_{\mathcal{T}} \in \text{NE}_{g,D}$ or $\text{ND}_{g,D}$ as follows:

$$\hat{\boldsymbol{\rho}}_{\mathcal{T}} = \sum_{F \in \mathcal{E}} \hat{\boldsymbol{\rho}}_F. \tag{3.16}$$

Based on the recovered gradient we define the local element based indicators and global estimator related to the gradient recovery by

$$\eta_{\rho,K} = \left\| A^{1/2} (\hat{\boldsymbol{\rho}}_{\mathcal{T}} - \tilde{\boldsymbol{\rho}}_{\mathcal{T}}) \right\|_{0,K}, \quad \forall K \in \mathcal{T} \quad \text{and} \quad \eta_\rho = \left\| A^{1/2} (\hat{\boldsymbol{\rho}}_{\mathcal{T}} - \tilde{\boldsymbol{\rho}}_{\mathcal{T}}) \right\|_{0,\Omega}, \tag{3.17}$$

respectively.

3.2. Flux recovery

Denote the $H(\text{div}, \Omega)$ conforming Raviart-Thomas (RT) and Brezzi-Douglas-Marini (BDM) spaces of the lowest index by

$$\text{RT} = \{ \boldsymbol{\tau} \in H(\text{div}; \Omega) : \boldsymbol{\tau}|_K \in \text{RT}(K) \ \forall K \in \mathcal{T} \}$$

$$\text{and BDM} = \{ \boldsymbol{\tau} \in H(\text{div}; \Omega) : \boldsymbol{\tau}|_K \in \text{BDM}(K) \ \forall K \in \mathcal{T} \},$$

respectively, where $RT(K) = \mathbb{P}_0(K)^2 + (x_1, x_2)\mathbb{P}_0(K)$ and $\text{BDM}(K) = \mathbb{P}_1(K)^d$. Let

$$\text{RT}_{g,N} = \text{RT} \cap H_{g,N}(\text{div}; \Omega) \quad \text{and} \quad \text{BDM}_{g,N} = \text{BDM} \cap H_{g,N}(\text{div}; \Omega).$$

Using the numerical flux $\tilde{\boldsymbol{\sigma}}_{\mathcal{T}} := -A\nabla u_{\mathcal{T}}$, we may reconstruct a flux

$$\hat{\boldsymbol{\sigma}}_{\mathcal{T}} \in \text{RT}_{g,N} \quad \text{or} \quad \text{BDM}_{g,N} \tag{3.18}$$

by employing the same procedure introduced in [5]. The corresponding local element based indicators and global estimator are then defined by

$$\eta_{\sigma,K} = \left\| A^{-1/2} (\hat{\boldsymbol{\sigma}}_{\mathcal{T}} - \tilde{\boldsymbol{\sigma}}_{\mathcal{T}}) \right\|_{0,K}, \quad \forall K \in \mathcal{T} \quad \text{and} \quad \eta_\sigma = \left\| A^{-1/2} (\hat{\boldsymbol{\sigma}}_{\mathcal{T}} - \tilde{\boldsymbol{\sigma}}_{\mathcal{T}}) \right\|_{0,\Omega}, \tag{3.19}$$

respectively.

3.3. Error estimators

For the Crouziex-Raviart finite element solution u^{cr}, the local error indicators and global estimator are defined by

$$\eta_K^{cr} = \left(\left(\eta_{\sigma,K} \right)^2 + \left(\eta_{\rho,K} \right)^2 \right)^{1/2}, \quad \forall K \in \mathcal{T} \quad \text{and} \quad \eta_{cr} = \left(\sum_{K \in \mathcal{T}} \left(\eta_K^{cr} \right)^2 \right)^{1/2}, \tag{3.20}$$

respectively. For the DG finite element solution u^{dg}, the local error indicators and global estimator are defined by

$$\tilde{\eta}_K^{dg} = \left(\left(\eta_{\sigma,K} \right)^2 + \left(\eta_{\rho,K} \right)^2 \right)^{1/2}, \quad \forall K \in \mathcal{T} \quad \text{and} \quad \tilde{\eta}_{dg} = \left(\sum_{K \in \mathcal{T}} \left(\tilde{\eta}_K^{dg} \right)^2 \right)^{1/2}, \tag{3.21}$$

respectively. Unfortunately, we are not able to establish its reliability bound due to the lack of equivalence between the solution jumps across neighboring elements and the $\eta_{\rho,K}$'s. For theoretical reason, we also consider the following local error indicators and global estimator that simply replaces $\eta_{\rho,K}$ by the jumps of solutions:

$$\eta_K^{dg} = \left(\eta_{\sigma,K}^2 + \sum_{F \in \mathcal{E}_I \cup \mathcal{E}_K} \frac{1}{2} \left| u^{dg} \right|_{j,F}^2 + \sum_{F \in \mathcal{E}_D \cup \mathcal{E}_K} \left| u^{dg} \right|_{j,F}^2 \right)^{1/2}, \ \forall K \in \mathcal{T} \text{ and } \eta_{dg} = \left(\sum_{K \in \mathcal{T}} \left(\eta_K^{dg} \right)^2 \right)^{1/2}, \tag{3.22}$$

respectively.

Remark 3.1. By an inverse inequality, it can be easily seen that $\tilde{\eta}_K^{dg} \lesssim \eta_K^{dg}$. In our numerical results, the estimators η^{dg} and $\tilde{\eta}^{dg}$ (see Figs. 6 and 10) are very close for the first order discontinuous finite element method.

4. Reliability and efficiency

This section establishes efficiency and reliability bounds of the indicators and estimators defined in (3.20) and (3.22), for the diffusion problem with the coefficient matrix A satisfying the mildly anisotropic assumption.

Define the jumps of the tangential component of the gradient and the normal component of the flux on edges by

$$j_{t,F} = \begin{cases} [\![\nabla_h u_{\mathcal{T}} \cdot \mathbf{t}_F]\!], & \forall F \in \mathcal{E}_I, \\ 0, & \forall F \in \mathcal{E}_N, \text{ and} \\ \nabla_h u_{\mathcal{T}} \cdot \mathbf{t}_F - g'_{D,F}, & \forall F \in \mathcal{E}_D, \end{cases} \quad j_{n,F} = \begin{cases} [\![A\nabla_h u_{\mathcal{T}} \cdot \mathbf{n}_F]\!], & \forall F \in \mathcal{E}_I, \\ A\nabla_h u_{\mathcal{T}} \cdot \mathbf{n}_F - g_{N,F}, & \forall F \in \mathcal{E}_N, \\ 0, & \forall F \in \mathcal{E}_D. \end{cases}$$

Lemma 4.1. Let $u_{\mathcal{T}}$ be the finite element solution of (2.5) or (2.7), and let $\hat{\boldsymbol{\sigma}}_{\mathcal{T}}$ and $\hat{\boldsymbol{\rho}}_{\mathcal{T}}$ be the recovered flux and gradient from $u_{\mathcal{T}}$ given in (3.16) and (3.18), respectively. Then the following results hold

$$\left(\sum_{F \in \mathcal{E}_I \cup \mathcal{E}_D} h_F \alpha_{F,H} \left\| j_{t,F} \right\|_{0,F}^2 \right)^{1/2} \le C \left\| A^{1/2} (\hat{\boldsymbol{\rho}}_{\mathcal{T}} - \tilde{\boldsymbol{\rho}}_{\mathcal{T}}) \right\|_{0,\Omega}, \tag{4.23}$$

and

$$\left(\sum_{F \in \mathcal{E}_I \cup \mathcal{E}_N} \frac{h_F}{\alpha_{F,A}} \left\| j_{n,F} \right\|_{0,F}^2 \right)^{1/2} \le C \left\| A^{-1/2} (\hat{\boldsymbol{\sigma}}_{\mathcal{T}} - \tilde{\boldsymbol{\sigma}}_{\mathcal{T}}) \right\|_{0,\Omega}, \tag{4.24}$$

where the positive constant C depends on the shape regularity of $\mathcal{T}$ and κ, but not on $\frac{\lambda_{\max}}{\lambda_{\min}}$.

Proof. To the validity of (4.23), it suffices to prove that

$$h_F^{1/2} \alpha_{F,H}^{1/2} \left\| j_{t,F} \right\|_{0,F} \le C \left\| A^{1/2} (\hat{\boldsymbol{\rho}}_{\mathcal{T}} - \tilde{\boldsymbol{\rho}}_{\mathcal{T}}) \right\|_{0,\omega_F}, \quad \forall F \in \mathcal{E}_I \cup \mathcal{E}_D, \tag{4.25}$$

where $\omega_F = K_F^+ \cup K_F^-$. Without loss of generality, we prove (4.25) for each $F \in \mathcal{E}_I$. Applying the fact that $\|[\![\hat{\boldsymbol{\rho}}_F \cdot \mathbf{t}_F]\!]\|_{0,F} = 0$ for all $F \in \mathcal{E}_I$, the triangle, trace and inverse inequalities, and (2.4) yields

$$\begin{aligned} h_F^{1/2} \alpha_{F,H}^{1/2} \left\| j_{t,F} \right\|_{0,F} &= h_F^{1/2} \alpha_{F,H}^{1/2} \|[\![\tilde{\boldsymbol{\rho}}_{\mathcal{T}} - \hat{\boldsymbol{\rho}}_{\mathcal{T}}]\!] \cdot \mathbf{t}_F\|_{0,F} \\ &\le h_F^{1/2} \alpha_{F,H}^{1/2} \left(\left\| (\hat{\boldsymbol{\rho}}_{\mathcal{T}} - \tilde{\boldsymbol{\rho}}_{\mathcal{T}})|_{K_F^-} \cdot \mathbf{t}_F \right\|_{0,F} + \left\| (\hat{\boldsymbol{\rho}}_{\mathcal{T}} - \tilde{\boldsymbol{\rho}}_{\mathcal{T}})|_{K_F^+} \cdot \mathbf{t}_F \right\|_{0,F} \right) \\ &\le C \alpha_{F,H}^{1/2} \left(\left\| \hat{\boldsymbol{\rho}}_{\mathcal{T}} - \tilde{\boldsymbol{\rho}}_{\mathcal{T}} \right\|_{0,K_F^-} + \left\| \hat{\boldsymbol{\rho}}_{\mathcal{T}} - \tilde{\boldsymbol{\rho}}_{\mathcal{T}} \right\|_{0,K_F^+} \right) \\ &\le C \left(\left\| A^{1/2} (\hat{\boldsymbol{\rho}}_{\mathcal{T}} - \tilde{\boldsymbol{\rho}}_{\mathcal{T}}) \right\|_{0,K_F^-} + \left\| A^{1/2} (\hat{\boldsymbol{\rho}}_{\mathcal{T}} - \tilde{\boldsymbol{\rho}}_{\mathcal{T}}) \right\|_{0,K_F^+} \right). \end{aligned}$$

This completes the proof of (4.25) and, hence, (4.23). (4.24) may be proved in a similar fashion. This completes the proof of the lemma. □

4.1. Reliability and efficiency for the nonconforming method

Define

$$\eta_{res} = \left(\sum_{K \in \mathcal{T}} \frac{h_K^2}{\lambda_{max,K}} \| f_K \|_{0,K}^2 \right)^{1/2}$$

for the error related to the element residual where $f_K = f|_K$.

In the following theorem, we prove the reliability property for the CR element through the existing reliability result of a classical properly weighted residual based error estimation [4]. Doing this enables our estimators to inherit the unconditional robustness as the properly weighted residual based estimator.

Theorem 4.1. *The estimator η_{cr} defined in* (3.20) *satisfies the following reliability bound:*

$$\left\| A^{1/2} \nabla_h (u - u^{cr}) \right\|_{0,\Omega} \leq C \left(\eta_{cr}^2 + \eta_{res}^2 \right)^{1/2}, \tag{4.26}$$

where the positive constant C depends on the shape regularity of $\mathcal{T}$ and κ, but not on $\dfrac{\lambda_{\max}}{\lambda_{\min}}$.

Proof. Firstly, the residual based error estimator for CR elements reads that (see Theorem 3.5 in [4]) there exists a constant $C > 0$ that depends on the shape regularity of $\mathcal{T}$ and κ, but not on $\dfrac{\lambda_{\max}}{\lambda_{\min}}$ or the mesh size such that

$$\left\| A^{1/2} \nabla_h (u - u^{cr}) \right\|_{0,\Omega}$$

$$\leq C \left(\sum_{F \in \mathcal{E}_I \cup \mathcal{E}_D} \frac{\alpha_{F,H}}{h_F} \left\| [\![u_{\mathcal{T}}]\!] \right\|_{0,F}^2 + \sum_{F \in \mathcal{E}_I \cup \mathcal{E}_N} \frac{h_F}{\alpha_{F,A}} \left\| j_{n,F} \right\|_{0,F}^2 + (\eta_{res})^2 \right)^{1/2},$$

which, together with the fact that

$$\sqrt{\frac{\alpha_{F,H}}{h_F}} \left\| [\![u_{\mathcal{T}}]\!] \right\|_{0,F} = \sqrt{\frac{\alpha_{F,H} h_F}{12}} \left\| j_{t,F} \right\|_{0,F}, \quad \forall F \in \mathcal{E}_I \cup \mathcal{E}_D,$$

Lemma 4.1 and the Young's inequality, gives (4.26). This completes the proof the theorem. $\quad\square$

Remark 4.1. When the mesh size is relatively small, the element residual error can be eliminated in the error estimation (see, e.g., [12,7]). Numerical results without the element residual also exhibit a better approximation to the true error (see Fig. 8).

We now prove the local efficiency for the error indicator.

Theorem 4.2. *The local element-based indicators η_K^{cr} defined in* (3.20) *are efficient, i.e.,*

$$\eta_K^{cr} \leq C \left\| A^{1/2} \nabla_h (u - u^{cr}) \right\|_{0,\omega_K}, \quad \forall K \in \mathcal{T}, \tag{4.27}$$

where ω_K is the union of all elements that shares at least one edge with K and the positive constant C depends on the shape regularity of $\mathcal{T}$ and κ, but not on $\dfrac{\lambda_{\max}}{\lambda_{\min}}$ or the mesh size.

Proof. By the definition in (3.20),

$$\eta_K^{cr} = \left(\left\| A^{-1/2} (\hat{\boldsymbol{\sigma}}_{\mathcal{T}} - \tilde{\boldsymbol{\sigma}}_{\mathcal{T}}) \right\|_{0,K}^2 + \left\| A^{1/2} (\hat{\boldsymbol{\rho}}_{\mathcal{T}} - \tilde{\boldsymbol{\rho}}_{\mathcal{T}}) \right\|_{0,K}^2 \right)^{1/2}.$$

It follows from (3.13), (3.16), and the triangle inequality that

$$\left\| A^{1/2} (\hat{\boldsymbol{\rho}}_{\mathcal{T}} - \tilde{\boldsymbol{\rho}}_{\mathcal{T}}) \right\|_{0,K} \leq \sum_{F \in \mathcal{E}_K} \left\| A^{1/2} (\hat{\boldsymbol{\rho}}_F - \tilde{\boldsymbol{\rho}}_F) \right\|_{0,K} \leq \sum_{F \in \mathcal{E}_K} \left\| A^{1/2} (\hat{\boldsymbol{\rho}}_F - \tilde{\boldsymbol{\rho}}_F) \right\|_{0,\omega_F}. \tag{4.28}$$

Without loss of generality, assume that K is an interior element and that $\alpha_F^- \leq \alpha_F^+$ for each $F \in \mathcal{E}_K$. By (3.15), the mildly anisotropic assumption on A, and the facts that

$$\tilde{\rho}_F^+ |F| \boldsymbol{\zeta}_F \in \mathcal{V}_F = \mathrm{NE}_F \text{ or } \mathrm{ND}_F \quad \text{and} \quad \|\boldsymbol{\zeta}_F\|_{0,K_F^-} \leq C,$$

we have

$$\left\| A^{1/2}(\hat{\boldsymbol{\rho}}_F - \tilde{\boldsymbol{\rho}}_F) \right\|_{0,\omega_F} = \min_{\boldsymbol{\tau} \in \mathcal{V}_F} \left\| A^{1/2}(\boldsymbol{\tau} - \tilde{\boldsymbol{\rho}}_F) \right\|_{0,\omega_F}$$

$$\leq \left\| A^{1/2}\left(\tilde{\rho}_F^+ |F|\boldsymbol{\zeta}_F - \tilde{\boldsymbol{\rho}}_F\right) \right\|_{0,\omega_F} = \left\| A^{1/2}(\tilde{\rho}_F^+ - \tilde{\rho}_F^-)|F|\boldsymbol{\zeta}_F \right\|_{0,K_F^-} \tag{4.29}$$

$$\leq C \sqrt{\alpha_{F,H} h_F} \| j_{t,F} \|_{0,F}.$$

We also have the following classical efficiency bound for the tangential jump on edges (see e.g., Theorem 5.1 in [6]):

$$\sqrt{\alpha_{F,H} h_F} \| j_{t,F} \|_{0,F} \leq C \left\| A^{1/2} \nabla_h (u - u^{cr}) \right\|_{0,\omega_F}, \quad \forall F \in \mathcal{E}_I \cup \mathcal{E}_N. \tag{4.30}$$

Combining (4.28) - (4.30) gives

$$\left\| A^{1/2}(\hat{\boldsymbol{\rho}}_{\mathcal{T}} - \tilde{\boldsymbol{\rho}}_{\mathcal{T}}) \right\|_{0,K} \leq C \left\| A^{1/2} \nabla_h (u - u^{cr}) \right\|_{0,\omega_K}, \quad \forall K \in \mathcal{T}. \tag{4.31}$$

Similarly, we can prove that

$$\left\| A^{-1/2}(\hat{\boldsymbol{\sigma}}_{\mathcal{T}} - \tilde{\boldsymbol{\sigma}}_{\mathcal{T}}) \right\|_{0,K} \leq C \left\| A^{1/2} \nabla_h (u - u^{cr}) \right\|_{0,\omega_K}. \tag{4.32}$$

(4.27) is then a direct consequence of (4.31) and (4.32). This completes the proof of the theorem. □

4.2. Reliability and efficiency for the linear discontinuous Galerkin method

To prove the estimator reliability for DG element, we again use the classical weighted residual based error estimator as a bridge in order to inherit the unconditional robustness.

Theorem 4.3. *Let $u \in H^1(\Omega)$ and u^{dg} be the solution of (2.1) and (2.7), respectively. Then the estimator η_{dg} for the discontinuous element approximation satisfies the following robust reliability bound:*

$$\left\| u - u^{dg} \right\|_{dg,\Omega} \leq C \eta_{dg}, \tag{4.33}$$

where the positive constant C depends on the shape regularity of $\mathcal{T}$ and κ, but not on $\frac{\lambda_{\max}}{\lambda_{\min}}$.

Proof. For the residual based error estimator, we have the following reliability result (see Theorem 4.3 in [4]):

$$\| A^{1/2} \nabla(u - u^{dg}) \|_{0,\Omega} \leq C \left(\sum_{F \in \mathcal{E}_I \cup \mathcal{E}_D} \left| u^{dg} \right|_{j,F}^2 + \sum_{F \in \mathcal{E}_I \cup \mathcal{E}_N} \frac{h_F}{\alpha_{F,A}} \| j_{n,F} \|_{0,F}^2 \right)^{1/2}, \tag{4.34}$$

where the positive constant C depends on the shape regularity of $\mathcal{T}$ and κ, but not on $\frac{\lambda_{\max}}{\lambda_{\min}}$. The theorem is then a direct consequence of the (4.34) and Lemma 4.1. □

Theorem 4.4. *The local element-based indicators η_K^{dg} and $\tilde{\eta}_K^{dg}$ defined in (3.22) are efficient, i.e.,*

$$\eta_K^{dg} \leq C \| u - u^{dg} \|_{dg,\omega_K} \tag{4.35}$$

and

$$\tilde{\eta}_K^{dg} \leq C \| u - u^{dg} \|_{dg,\omega_K}, \tag{4.36}$$

where the positive constant C depends on the shape regularity of $\mathcal{T}$ and κ, but not on $\frac{\lambda_{\max}}{\lambda_{\min}}$.

Proof. By the inverse inequality, we have that

$$\tilde{\eta}_K^{dg} \leq \eta_K^{dg} \quad \forall K \in \mathcal{T}.$$

It is therefore sufficient to prove (4.35). The rest of the theorem can be proved similarly to the Theorem 4.2. □

Remark 4.2. For both the nonconforming and DG methods, the a posteriori error estimation is robust with respect to the jump of the coefficient, i.e., both the reliability and efficiency constants are both independent of $\frac{\lambda_{\max}}{\lambda_{\min}}$, regardless of its distribution.

5. Explicit formulas

In this section we present the explicit formulas for the recovered gradient in (3.16) and its corresponding error indicators and estimator in (3.17). For simplicity we assume that $A = \alpha I$ where α is piecewise constant. The formula can be easily updated for A being a matrix tensor. The quantities of interest are explicitly expressed in terms of the numerical solution and the geometric information of the mesh. It is easy to see that the recovered gradient is a weighted average of the numerical gradient. The overall explicit computation confirms the easy implementation and low computing cost.

Given an edge $F \in \mathcal{E}$ denote by $\mathbf{x}_F^{\pm}$ the opposite vertices of F in $K_F^{\pm}$, respectively. Given a vector $\mathbf{v} = (v_1, v_2)$, let $\mathbf{v}^{\perp} = (-v_2, v_1)$. Denote by $\lambda_{\mathbf{s}_F}$ and $\lambda_{\mathbf{e}_F}$ the nodal basis functions of the continuous linear element associated with vertices $\mathbf{s}_F$ and $\mathbf{e}_F$, respectively.

5.1. Formulas for the recovered gradient in $NE_{g,D}$

For the NE space of the lowest index, the nodal basis function associated with $F \in \mathcal{E}$ is given by

$$\zeta_F = \lambda_{\mathbf{s}_F} \nabla \lambda_{\mathbf{e}_F} - \lambda_{\mathbf{e}_F} \nabla \lambda_{\mathbf{s}_F}$$

which satisfies

$$\zeta_F \cdot \mathbf{t}_{F'} = |F|^{-1} \delta_{FF'}.$$

For all $F \in \mathcal{E}_I$, let

$$\gamma_F^{ne,\pm} = \left(\alpha \zeta_F, \zeta_F\right)_{K_F^{\pm}} \quad \text{and} \quad w_F^{ne} = \frac{\gamma_F^{ne,-}}{\gamma_F^{ne,-} + \gamma_F^{ne,+}}.$$

Using the basis function ζ_F defined above, a straightforward calculation gives

$$\gamma_F^{ne,\pm} = \frac{1}{48|K_F^{\pm}|} \left(\sum_{F' \subset \partial K_F^{\pm}} \left\| \alpha^{1/2} \left(\mathbf{x}_{F'}^{\pm} - \mathbf{x}_F^{\pm}\right)^{\perp} \right\|^2 + \left\| \alpha^{1/2} \left(\sum_{F' \subset \partial K_F^{\pm}} \mathbf{x}_{F'}^{\pm} - 3\mathbf{x}_F^{\pm} \right)^{\perp} \right\|^2 \right).$$

Recall that solving the local problem in (3.15) with $\mathcal{V}_F = NE_F$ yields the following representation for the recovered gradient in $NE_{g,D}$:

$$\hat{\boldsymbol{\rho}}_{\mathcal{T}}^{ne} = \sum_{F \in \mathcal{E}_I} \hat{\rho}_F \, |F| \zeta_F + \sum_{F \in \mathcal{E}_N} \tilde{\rho}_F \, |F| \zeta_F^- + \sum_{F \in \mathcal{E}_D} g_{D,F} |F| \zeta_F^-.$$

Now solving (3.15) gives that

$$\hat{\rho}_F = w_F^{ne} \, \tilde{\rho}_F^- + \left(1 - w_F^{ne}\right) \tilde{\rho}_F^+.$$

Note that the recovered gradient is indeed a weighted average of the numerical flux.

5.2. Formulas for the recovered gradient $ND_{g,D}$

For the ND space of the lowest index, two basis functions associated with the edge $F \in \mathcal{E}$ are given

$$\xi_{s,F} = \lambda_{\mathbf{s}_F} \nabla \lambda_{\mathbf{e}_F} \quad \text{and} \quad \xi_{e,F} = -\lambda_{\mathbf{e}_F} \nabla \lambda_{\mathbf{s}_F},$$

respectively, which satisfy

$$\left(\xi_{s,F} \cdot \mathbf{t}_{F'}\right)\Big|_{F'} = \lambda_{\mathbf{s}_F} \delta_{FF'}/|F| \quad \text{and} \quad \left(\xi_{e,F} \cdot \mathbf{t}_{F'}\right)\Big|_{F'} = \lambda_{\mathbf{e}_F} \delta_{FF'}/|F|$$

for any $F' \in \mathcal{E}$.

For all $F \in \mathcal{E}_I$ and for $i, j \in \{s, e\}$, let

$$\beta_{ij,F}^{nd,\pm} = \left(\alpha \xi_{i,F}, \xi_{j,F}\right)_{K_F^{\pm}} \quad \text{and} \quad \beta_{ij,F}^{nd} = \beta_{ij,F}^{nd,-} + \beta_{ij,F}^{nd,+},$$

and let

$$w_{s,F}^{nd} = \frac{\left(\beta_{ss,F}^{nd,-} + \beta_{se,F}^{nd,-}\right)\beta_{ee,F}^{nd} - \left(\beta_{se,F}^{nd,-} + \beta_{ee,F}^{nd,-}\right)\beta_{se,F}^{nd}}{\beta_{ss,F}^{nd}\beta_{ee,F}^{nd} - \left(\beta_{se,F}^{nd}\right)^2}$$

$$\text{and} \quad w_{e,F}^{nd} = \frac{\left(\beta_{se,F}^{nd,-} + \beta_{ee,F}^{nd,-}\right)\beta_{ss,F}^{nd} - \left(\beta_{ss,F}^{nd,-} + \beta_{se,F}^{nd,-}\right)\beta_{se,F}^{nd}}{\beta_{ss,F}^{nd}\beta_{ee,F}^{nd} - \left(\beta_{se,F}^{nd}\right)^2}.$$

Using the definition for basis functions $\boldsymbol{\xi}_{s,F}$ and $\boldsymbol{\xi}_{e,F}$, a straightforward calculation gives that

$$\beta_{ss,F}^{nd,\pm} = \frac{1}{24|K_F^{\pm}|}\left\|\alpha^{1/2}(\mathbf{x}_F^{\pm} - \mathbf{s}_F)^{\perp}\right\|^2, \quad \beta_{ee,F}^{nd,\pm} = \frac{1}{24|K_F^{\pm}|}\left\|\alpha^{1/2}(\mathbf{x}_F^{\pm} - \mathbf{e}_F)^{\perp}\right\|^2$$

$$\text{and} \quad \beta_{se,F}^{nd,\pm} = \frac{\left((\mathbf{x}_F^{\pm} - \mathbf{s}_F)^{\perp}\right)^t \alpha_K (\mathbf{x}_F^{\pm} - \mathbf{e}_F)^{\perp}}{48\,|K_F^{\pm}|}.$$

Recall that solving the local problems in (3.15) with $\mathcal{V}_F = \mathrm{ND}_F$ yields the following representation for the recovered gradient in ND_D:

$$\hat{\boldsymbol{\rho}}_{\mathcal{T}}^{nd} = \sum_{F \in \mathcal{E}_I}\left(\hat{\rho}_{s,F}\,\boldsymbol{\xi}_{s,F} + \hat{\rho}_{e,F}\,\boldsymbol{\xi}_{e,F}\right)|F| + \sum_{F \in \mathcal{E}_N}\tilde{\rho}_F\,|F|\boldsymbol{\zeta}_F^- + \sum_{F \in \mathcal{E}_D}g_{D,F}'|F|\boldsymbol{\zeta}_F^-.$$

Now solving (3.15) gives that

$$\hat{\rho}_{s,F} = w_{s,F}^{nd}\,\tilde{\rho}_F^- + \left(1 - w_{s,F}^{nd}\right)\tilde{\rho}_F^+ \quad \text{and} \quad \hat{\rho}_{e,F} = w_{e,F}^{nd}\,\tilde{\rho}_F^- + \left(1 - w_{e,F}^{nd}\right)\tilde{\rho}_F^+.$$

6. Numerical experiments

In this section, we report numerical results for the Kellogg [3] and L-shaped benchmark test problems approximated by the Crouziex-Raviart and DG finite element methods.

Example 1 *(Kellogg's problem).* Let $\Omega = (-1, 1)^2$ and

$$u(r, \theta) = r^{\beta}\mu(\theta)$$

in the polar coordinates at the origin with

$$\mu(\theta) = \begin{cases} \cos((\pi/2 - \sigma)\beta) \cdot \cos((\theta - \pi/2 + \rho)\beta) & \text{if} \quad 0 \le \theta \le \pi/2, \\ \cos(\rho\beta) \cdot \cos((\theta - \pi + \sigma)\beta) & \text{if} \quad \pi/2 \le \theta \le \pi, \\ \cos(\sigma\beta) \cdot \cos((\theta - \pi - \rho)\beta) & \text{if} \quad \pi \le \theta \le 3\pi/2, \\ \cos((\pi/2 - \rho)\beta) \cdot \cos((\theta - 3\pi/2 - \sigma)\beta) & \text{if} \quad 3\pi/2 \le \theta \le 2\pi, \end{cases}$$

where σ and ρ are numbers. The function $u(r, \theta)$ satisfies the diffusion equation in (2.1) with $A = \alpha I$, $\Gamma_N = \emptyset$, $f = 0$, and

$$\alpha = \begin{cases} R & \text{in } (0, 1)^2 \cup (-1, 0)^2, \\ 1 & \text{in } \Omega \setminus ([0, 1]^2 \cup [-1, 0]^2). \end{cases}$$

In the test problem, we choose $\beta = 0.1$ which is corresponding to

$$R \approx 161.4476387975881, \quad \rho = \frac{\pi}{4}, \quad \text{and} \quad \sigma \approx -14.92256510455152.$$

Note that the solution $u(r, \theta)$ is only in $H^{1+\beta-\epsilon}(\Omega)$ for some $\epsilon > 0$ and, hence, it is very singular for small β at the origin. This suggests that refinements should be centered mostly around the origin.

In the adaptive mesh refinement (AMR) procedure, we first use the Crouziex-Raviart nonconforming finite element method with indicators given in (3.20) and set the stopping criteria such that the relative error (the ratio between the energy norms of the true error and the true solution) less than 10%. We start with a uniform mesh with 8 elements (right diagonal). In each step, we mark all elements with the top 10% error. Each marked element is then divided into four elements by joining its mid-points. Necessary further steps are performed to remove the hanging nodes. Note that for the Kellogg problem $\eta_{\sigma,K}$ vanishes because $f = 0$ (see [20]). Then for the Kellogg problem, we have
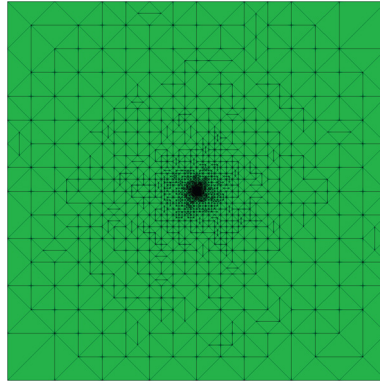
Fig. 1. Example 1. Mesh generated by η_K^{cr}.
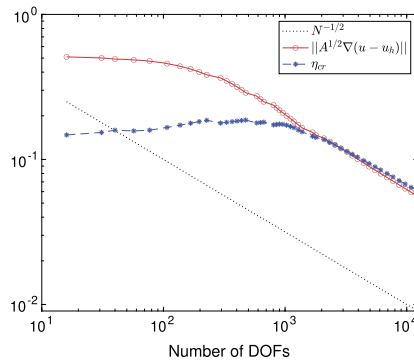
Fig. 2. Example 1. Comparison between true error and estimator η^{cr}.
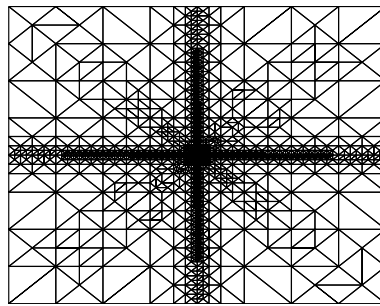
Fig. 3. Example 1. Mesh generated by $\eta_{zz,K}^{\rho}$.

$$\eta_K = \eta_{\rho,K}, \quad \forall K \in \mathcal{T}.$$

With the recovered gradient in the NE space, the final mesh is obtained at the 47th step, see Fig. 1. The refinements are centered around the origin and there is no over refinement along the interfaces. The comparison between the true error in the energy norm and the error estimator based on the recovered gradient in the NE space is shown in the log-log plot (see Fig. 2). The slope of the $\dfrac{\log(\text{error})}{\log(\text{number of dofs})}$ for both the estimator and the energy norm of the true error is very close to $-1/2$, which indicates the optimal decay of the error with respect to the number of the unknowns. The efficiency index is defined by

$$\text{eff-index} = \frac{\eta}{\|A^{1/2}\nabla(u - u_{\mathcal{T}})\|_{0,\Omega}},$$

where η is the estimator. The efficiency index of the estimator is approximately equal to 1.08. Recovering a gradient in the ND space produces very similar results.
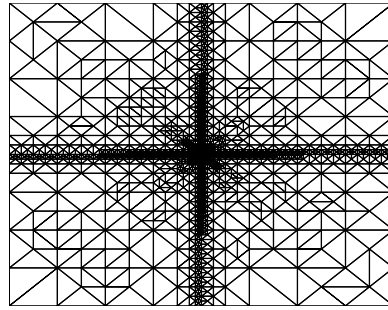
Fig. 4. Example 1. Mesh generated by $\eta_{zz,K}^{\sigma}$.
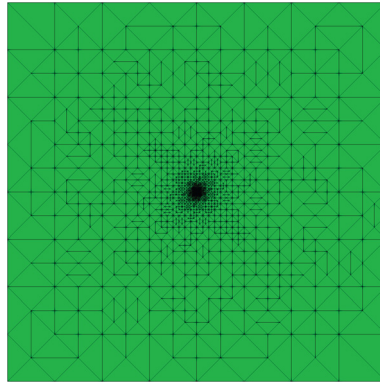
Fig. 5. Example 1. Mesh generated by $\tilde{\eta}_K^{dg}$.
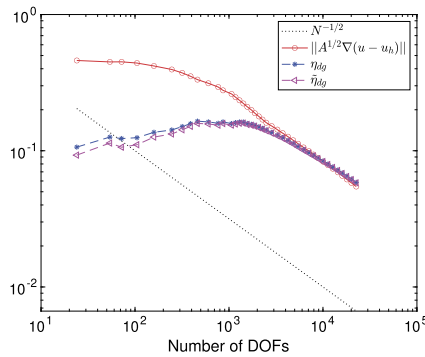
Fig. 6. Example 1. Comparison between true error and estimators.

Now we compare our error estimator with the classical ZZ error estimator that recover the flux and gradient in the continuous spaces. Let $\boldsymbol{\rho}_{zz}$ and $\boldsymbol{\sigma}_{zz}$ be the L^2 projection of the respective numerical gradient $\tilde{\boldsymbol{\rho}}_{\mathcal{T}}$ and flux $\tilde{\boldsymbol{\sigma}}_{\mathcal{T}}$ in the continuous piecewise linear space, i.e.,

$$(\boldsymbol{\rho}_{zz}, \mathbf{v}) = (\tilde{\boldsymbol{\rho}}_{\mathcal{T}}^{cr}, \mathbf{v}) \quad \text{and} \quad (\boldsymbol{\sigma}_{zz}, \mathbf{v}) = (\tilde{\boldsymbol{\sigma}}_{\mathcal{T}}^{cr}, \mathbf{v}) \quad \forall \mathbf{v} \in \mathbb{P}^1(\mathcal{T})^2,$$

where $\mathbb{P}^1(\mathcal{T}) = \{v \in H^1(\Omega) : v|_K \in \mathbb{P}^1(K) \; \forall K \in \mathcal{T}\}$. We then define the corresponding error estimators as

$$\eta_{\rho,K}^{zz} = \|A^{1/2}(\boldsymbol{\rho}_{zz} - \tilde{\boldsymbol{\rho}}_{\mathcal{T}}^{cr})\|_K \quad \text{and} \quad \eta_{\sigma,K}^{zz} = \|A^{-1/2}(\boldsymbol{\sigma}_{zz} - \tilde{\boldsymbol{\sigma}}_{\mathcal{T}}^{cr})\|_K, \quad \forall K \in \mathcal{T}.$$

Figs. 3 and 4 show the meshes generated by the respective $\eta_{\rho,K}^{zz}$ and $\eta_{\sigma,K}^{zz}$. It can be seen that unnecessary refinements are added along the entire interfaces. This is due to the artificial error created by enforcing the flux and gradient into the continuous space while the true ones are not continuous.

We also present numerical results for the Kellogg problem using the DG method. We choose $\gamma = 50$ in (2.8) for this example. Due to the big jump of the diffusion coefficient, γ value should be big enough to ensure the stability of the numerical scheme. With the same stopping criteria, the final mesh generated by $\tilde{\eta}_K^{dg}$ and obtained at the 40th step is given
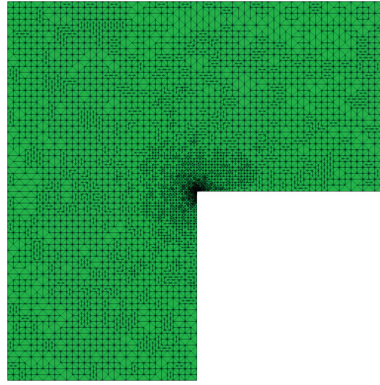
Fig. 7. Example 2. Mesh generated by η_K^{cr}.
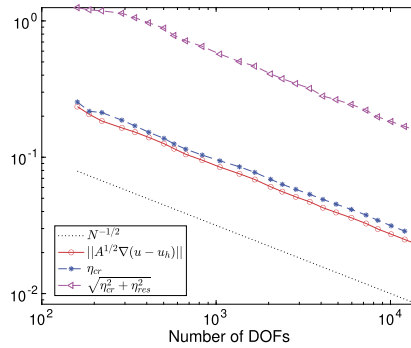
Fig. 8. Example 2. Comparison between true error and estimators.
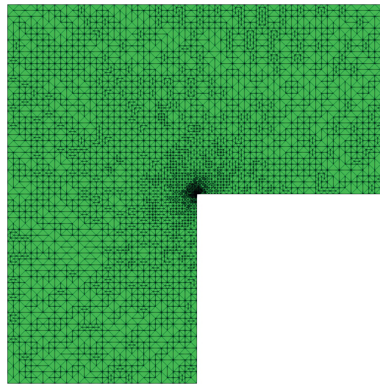
Fig. 9. Example 2. Mesh generated by $\tilde{\eta}_K^{dg}$.

in Fig. 5. We used the recovered flux and gradient in the respective RT and NE spaces. Again, refinements are centered around the origin and there is no over refinement along the interface. The efficiency index for the $\tilde{\eta}_K^{dg}$ is around 1.07. The quantities η^{dg} and $\tilde{\eta}^{dg}$ for the linear case are very close. This indicates that, numerically, $\tilde{\eta}^{dg}$ is a good error estimator. Numerical results using BDM and ND spaces to recover the flux and gradient are very similar.

Example 2 *(L-shape problem).* In this example, we test the following problem:

$$u(r, \theta) = r^{2/3} \sin(2\theta/3) + r^2/2, \quad \theta \in [0, 3\pi/2]$$

on the L-shaped domain $\Omega = (-1, 1)^2 \setminus [0, 1] \times [-1, 0]$. Note that this function satisfies (2.1) with $A(x) = I$ and $f = -2$.

We again test both the Crouzeix-Raviart and DG methods. For the DG method, we set $\gamma = 10$ in (2.8). We start with an initial uniform mesh with 96 elements (right diagonal). With the stopping criteria that the relative error be less than
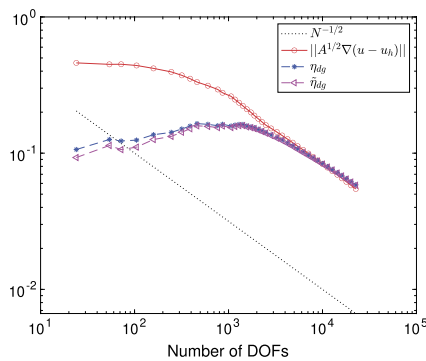
Fig. 10. Example 2. Comparison between true error and estimators.

one percent, the meshes generated by the indicator η_K^{cr} and $\tilde{\eta}_K^{dg}$ with the recovered gradient and flux in the respective NE and RT spaces are depicted in Figs. 7 and 9, respectively. It takes 25 steps for the Crouzeix-Raviart method and 23 steps for the DG method to reach the stopping criteria. The problem has an angular singularity around the origin and we observe that refinements are much more dense around the singular point. The corresponding comparisons between the true error in the energy norm and the error estimators are shown in the log-log Figs. 8 and 10. All estimators converge with the optimal order. The estimator has the efficiency index around 1.15 for η_{cr} and 1.09 for $\tilde{\eta}_{dg}$. In Fig. 8, we also compare the estimator $\sqrt{\eta_{cr}^2 + \eta_{res}^2}$ for the Crouzeix-Raviart method. Its efficiency index is around 6.80 which makes it a less effective error estimator. Again, for the DG method the quantities η^{dg} and $\tilde{\eta}^{dg}$ are very close.

References

[1] M. Ainsworth, Robust a posteriori error estimation for nonconforming finite element approximation, SIAM J. Numer. Anal. 42 (6) (2005) 2320–2341.
[2] M. Ainsworth, A posteriori error estimation for discontinuous Galerkin finite element approximation, SIAM J. Numer. Anal. 45 (4) (2007) 1777–1798.
[3] R. Bruce Kellogg, On the Poisson equation with intersecting interfaces, Appl. Anal. 4 (2) (1974) 101–129.
[4] Z. Cai, C. He, S. Zhang, Discontinuous finite element methods for interface problems: robust a priori and a posteriori error estimates, SIAM J. Numer. Anal. 55 (1) (2017) 400–418.
[5] Z. Cai, C. He, S. Zhang, Improved zz a posteriori error estimators for diffusion problems: conforming linear elements, Comput. Methods Appl. Mech. Eng. 313 (2017) 433–449.
[6] Z. Cai, C. He, S. Zhang, Residual-based a posteriori error estimate for interface problems: nonconforming linear elements, Math. Comput. 86 (304) (2017) 617–636.
[7] Z. Cai, X. Ye, S. Zhang, Discontinuous Galerkin finite element methods for interface problems: a priori and a posteriori error estimations, SIAM J. Numer. Anal. 49 (5) (2011) 1761–1787.
[8] Z. Cai, S. Zhang, Recovery-based error estimator for interface problems: conforming linear elements, SIAM J. Numer. Anal. 47 (3) (2009) 2132–2156.
[9] Z. Cai, S. Zhang, Recovery-based error estimators for interface problems: mixed and nonconforming finite elements, SIAM J. Numer. Anal. 48 (1) (2010) 30–52.
[10] Z. Cai, S. Zhang, Robust equilibrated residual error estimator for diffusion problems: conforming elements, SIAM J. Numer. Anal. 50 (1) (2012) 151–170.
[11] C. Carstensen, S. Bartels, R. Klose, An experimental survey of a posteriori courant finite element error control for the Poisson equation, Adv. Comput. Math. 15 (1–4) (2001) 79–106.
[12] C. Carstensen, R. Verfürth, Edge residuals dominate a posteriori error estimates for low order finite element methods, SIAM J. Numer. Anal. 36 (5) (1999) 1571–1587.
[13] B. Cockburn, W. Zhang, A posteriori error estimates for hdg methods, J. Sci. Comput. 51 (3) (2012) 582–607.
[14] M. Costabel, A coercive bilinear form for Maxwell's equations, J. Math. Anal. Appl. 157 (2) (1991) 527–541.
[15] M. Crouzeix, P.-A. Raviart, Conforming and nonconforming finite element methods for solving the stationary Stokes equations i, Modél. Math. Anal. Numér. 7 (R3) (1973) 33–75.
[16] A. Ern, S. Nicaise, M. Vohralík, An accurate h (div) flux reconstruction for discontinuous Galerkin approximations of elliptic problems, C. R. Math. 345 (12) (2007) 709–712.
[17] A. Ern, M. Vohralík, Polynomial-degree-robust a posteriori estimates in a unified setting for conforming, nonconforming, discontinuous Galerkin, and mixed discretizations, SIAM J. Numer. Anal. 53 (2) (2015) 1058–1081.
[18] W. Hoffmann, A. Schatz, L. Wahlbin, G. Wittum, Asymptotically exact a posteriori estimators for the pointwise gradient error on each element in irregular meshes. Part 1: a smooth problem and globally quasi-uniform meshes, Math. Comput. 70 (235) (2001) 897–909.
[19] K.-Y. Kim, Flux reconstruction for the p2 nonconforming finite element method with application to a posteriori error estimation, Appl. Numer. Math. 62 (12) (2012) 1701–1717.
[20] L.D. Marini, An inexpensive method for the evaluation of the solution of the lowest order Raviart–Thomas mixed method, SIAM J. Numer. Anal. 22 (3) (1985) 493–496.
[21] M. Petzoldt, A posteriori error estimators for elliptic equations with discontinuous coefficients, Adv. Comput. Math. 16 (1) (2002) 47–75.
[22] B. Riviere, M.F. Wheeler, A posteriori error estimates for a discontinuous Galerkin method applied to elliptic problems. log number: R74, Comput. Math. Appl. 46 (1) (2003) 141–163.
[23] R. Rodríguez, Some remarks on Zienkiewicz-Zhu estimator, Numer. Methods Partial Differ. Equ. 10 (5) (1994) 625–635.
[24] A. Schatz, L. Wahlbin, Asymptotically exact a posteriori estimators for the pointwise gradient error on each element in irregular meshes. Part ii: the piecewise linear case, Math. Comput. 73 (246) (2004) 517–523.
[25] Z. Zhang, A posteriori error estimates on irregular grids based on gradient recovery, Adv. Comput. Math. 15 (1–4) (2001) 363–374.
[26] Z. Zhang, Recovery techniques in finite element methods, Adapt. Comput. Theory Algorithms 6 (2007) 333–412.

[27] Z. Zhang, J. Zhu, Analysis of the superconvergent patch recovery technique and a posteriori error estimator in the finite element method (i), Comput. Methods Appl. Mech. Eng. 123 (1) (1995) 173–188.
[28] Z. Zhang, J. Zhu, Analysis of the superconvergent patch recovery technique and a posteriori error estimator in the finite element method (ii), Comput. Methods Appl. Mech. Eng. 163 (1) (1998) 159–170.
[29] O.C. Zienkiewicz, J.Z. Zhu, A simple error estimator and adaptive procedure for practical engineering analysis, Int. J. Numer. Methods Eng. 24 (2) (1987) 337–357.
[30] O.C. Zienkiewicz, J.Z. Zhu, The superconvergent patch recovery and a posteriori error estimates. Part 1: the recovery technique, Int. J. Numer. Methods Eng. 33 (7) (1992) 1331–1364.
[31] O.C. Zienkiewicz, J.Z. Zhu, The superconvergent patch recovery and a posteriori error estimates. Part 2: error estimates and adaptivity, Int. J. Numer. Methods Eng. 33 (7) (1992) 1365–1382.